Proceedings of the EUROCOALASH 2012 Conference,
Thessaloniki Greece, September 25-27 2012
http:// www.evipar.org/

"Alkaline Activation" as a procedure for the transformation of fly ashes into cementitious materials. Part II. Immobilisation of toxic and hazardous elements

S. Donatello[1], A. Fernández-Jiménez[2], and A. Palomo[3]

[1] Eduardo Torroja Institute (CSIC), Serrano Galvache Nº 4, 28033 Madrid, Spain, email: shanedonatello@ietcc.csic.es
[2] Eduardo Torroja Institute (CSIC), Serrano Galvache Nº 4, 28033 Madrid, Spain, email: anafj@ietcc.csic.es
[3] Eduardo Torroja Institute (CSIC), Serrano Galvache Nº 4, 28033 Madrid, Spain, email: palomo@ietcc.csic.es

Abstract

In this study, the potential of alkali activated fly ash cements to immobilise metals that are generally not well immobilised in Portland cements was examined. A class F fly ash was activated with a solution of 8M NaOH to form a hardened cementitious paste. Prior to activation, fly ashes were doped with either: *i)* 5000 mg/kg (0.5%) Hg^{2+} as $HgCl_2$, *ii)* 10000 mg/kg (1.0%) Cs^{+} as $CsOH.H_2O$ or *iii)* 10000 mg/kg (1.0%) As^{3+} as $NaAsO_2$. Mechanical strengths of the pastes were measured and the degree of metal immobilisation in pastes was determined by TCLP leaching tests. Finally, a study of the crystalline phases and paste microstructure was carried out to determine the fate of immobilised metals in the AAFA matrix.

Microstructural analysis of Hg doped pastes showed a strong correlation between Hg and S, implying that formation of highly insoluble HgS or Hg_2S precipitates is an important immobilisation mechanism. However, the coexistence of HgO could not be entirely ruled out. In Cs doped pastes, it is proposed that Cs^{+} ions are associated with the N-A-S-H gel and zeolites formed in AAFA cements, suggesting that Cs is mainly chemically bound rather than physically encapsulated. With As doped pastes, generally poor performance was observed, both with and without the addition of Fe_2O_3 in an attempt to improve immobilisation.

Keywords: fly ash, alkali activation, geopolymer, zeolite, Cesium, Mercury, Arsenic, TCLP, leaching.

1 Introduction

1.1. Alkali activated fly ash cements

Alkali activated fly ash (AAFA) cements are Portland cement free binders that consist entirely of coal fly ash as the solid starting material. The ashes are typically activated by a strongly alkaline NaOH solution with or without the addition of sodium silicate. Curing at a moderately elevated temperature leads to the formation of hardened pastes with high early strengths that can be used in mortars and concretes (see Figure 1).

During the setting and hardening process, the reactive aluminosilicates present in the fly ash release Al and Si to the liquid phase, which quickly precipitate into crosslinked, 3-D aluminosilicate tetrahedral networks (cementitious gel). In the tetrahedral co-ordination, aluminate groups carry a negative change, which is balanced by Na^{+} cations provided by the NaOH activator solution. This has led to the gel being referred to as N-A-S-H gel (in contrast to C-S-H gel with Portland cement, which consists of Ca, Si and

water). The N-A-S-H gel is XRD amorphous but if cured for very long periods at ambient temperature, or for slightly longer periods at elevated temperatures (<110°C), the gel transforms into one of several possible types of zeolite phase [1-5]. Such behaviour has led to the gel produced in AAFA cements being referred to as “zeolite precursors” in the literature.

1.2 Waste stabilisation and solidification of Cs, Hg and As

The landfill disposal of wastes containing high contents of heavy metals represents a significant risk of environmental contamination and as such, various leaching tests have been introduced in order to determine if a waste is suitable for landfill disposal, and if so, to which class of landfill site [6,7].

In problematic wastes, the most common method to reduce the solubility of heavy metals is to immobilise the waste in a Portland cement matrix. As the paste hardens, the heavy metals are physically inhibited from contact with the external environment (solidification). In the case of many heavy metals, they are also chemically converted to highly insoluble hydroxide salts (stabilisation) due to the alkaline nature of the cement pore solution.

However, not all metals can be stabilised successfully in a Portland cement matrix. For example, Cesium (Cs) is a highly soluble alkali-metal cation, which occurs in low and intermediate level radioactive wastes both as a by-product from nuclear fission and in medical wastes. Attempts to immobilise Cs in Portland cement matrices have produced generally unacceptable results. For example Bagosi and Csetenyi (1999) showed that Cs leaching from ion exchange resins loaded with ^{137}Cs actually increased by at least an order of magnitude after the resins were immobilised in Portland cement [8]. These authors found that Cs leaching could be significantly reduced by incorporating zeolites into the cement matrix.

Another element not well immobilised in Portland cement is Mercury (Hg). Under the alkaline environment of Portland cement, soluble Hg^{2+} ions are predicted to form sparingly soluble HgO salts instead of a highly insoluble hydroxide [9,10]. The long term stability of HgO in a cement matrix is uncertain in light of the results published by Hamilton and Bower (1997), which showed significant Hg vapour release from HgO immobilised in Portland cement [11]. In general little or no chemical interaction between Hg^{2+} and Portland cement hydration products is considered to take place [12].

Problems with the immobilisation of Arsenic (As) in Portland cement are well known and generally require highly specific conditions for good immobilisation [13-17]. Due to the amphoteric nature of As, this heavy metal can be highly soluble both at high and low pH´s. The incorporation of Iron, Iron oxides or Iron oxyhydroxides has been shown, in certain cases, to reduce As solubility [18,19].

Within the last 10 years, a number of studies regarding the use of AAFA cements as in the immobilisation of elements such as Arsenic, Boron, Lead, Cadmium, Cesium, Chromium and Mercury can be found in the literature [20-27]. It is worthwhile also considering that in many cases zeolites are specifically manufactured for heavy metal removal applications [28]. Numerous examples of zeolite-facilitated Arsenic, Caesium or Mercury removal can be found in the literature [29-35].

Given that AAFA cements can be considered as “zeolite precursors”, and that specially manufactured zeolites can show good removal of some metals which are not well immobilised by Portland cement, it is therefore of interest to review the immobilisation capacity of AAFA cements for Cs, Hg and As, which is the objective of this work.

2 Materials and methods

2.1 Materials

The fly ash used was of the class F variety and was activated with a solution of 8M NaOH prepared using reagent grade NaOH pellets. The metal salts were all reagent grade and added as either; $CsOH.H_2O$ $HgCl_2$ or $NaAsO_2$.

2.2 Paste preparation

Pastes were prepared using 100g batches of fly ash ground until ≥80% of the sample mass passed a 45μm sieve. In cases where heavy metals were to be mixed with the fly ash, the combined weight of metal salt and fly ash was maintained at 100g and blended for 30 minutes in a tumbling device to ensure sample homogeneity.

The dry fly ash or fly ash/salt mixtures were then mixed with 8M NaOH solution which had been prepared 24 hours earlier and cooled to room temperature. The liquid to solid ratio used was 0.4. Pastes were hand mixed for 3 minutes then cast into 1x1x6cm stainless steel moulds with the aid of a jolting apparatus. The moulds were then sealed in plastic bags and cured in an oven set at 85°C. The different mixtures studied are given in Table 1 below:

2.3 Mechanical strengths

The flexural strengths of the 1x1x6cm prisms were measured by a 3 point bending test (NET-ZSCH 6.111.2, GmbH). Compressive strengths of the two halves of each broken prism were then measured (Ibertest Autotest 200/10 SW).

2.4 Toxicity Characteristic Leaching Profile

The method employed was adapted from the US EPA method 1311. Broken fragments from strength tests in the size range 4.5 < 9.5mm were used. Preliminary testing of the acid neutralisation capacity of pastes required that the use of TCLP extraction fluid 2 in tests (Acetic acid at pH 2.88). The liquid to solid ratio used was 20:1 and the mixtures were agitated in an end over end shaker for 18 hours prior to filtration. The filtrates were acidified to pH <2 by the addition of an accurately known volume of 5M HNO_3 and metals concentrations were determined by ICP-AES.

2.5 Microstructural and crystalline phase analysis

Selected pastes were analysed by Mercury intrusion porosimetry (Micrometrics 9320) to determine the evolution in pore size distributions in pastes following curing at 85°C. Zeolite formation in the control paste was also examined by both X-Ray diffraction (XRD – Bruker D8 Advance) and scanning electron microscopy (SEM – Hitachi S4800). Selected pastes containing heavy metal additions were also analysed by XRD and/or SEM.

3 Results and discussion

3.1 Mechanical strength results

Compressive and flexural strength results are given in Figure 2, relative to the strengths of relevant control pastes that were prepared, cured and tested at the same times as test pastes.

From the results reported in Figure 2, it is clear that in all cases, the addition of Cs, Hg or As had an adverse impact on mechanical strengths of pastes. The addition of Hg had the least negative impact, which will be at least in part be due to the lower quantity of metal salt added. The largest drops in compressive strengths were associated with the addition of the As salt. The relative drop in strengths was virtually identical in As pastes both with and without the Fe_2O_3 addition. However, looking at Table 1, it is obvious that to achieve a 10000ppm dosage, more weight of As salt was required than Cs salt. This basic factor could have a significant influence on the strength drops in As doped pastes being greater than in Cs doped pastes. Another potential factor in favour of Cs over As is that the Cs salt used was the hydroxide, which is highly alkaline, unlike the $NaAsO_2$ salt.

Although high compressive strengths are not essential in solidification and stabilisation applications, such changes in strength, beyond the simple dilution effect, do hint at considerable changes in the sample

microstructure. Such changes could have potentially damaging consequences in terms of the long term durability of monoliths.

3.2 TCLP results

The immobilisation efficiencies of each of the metals in question are given in Table 2. Both Cs and Hg showed high degrees of immobilisation in the AAFA matrix. However, a large fraction (ca. 50%) of the As added to the fly ash remained in a soluble form. The addition of an excess of Iron oxide (5% by sample dry mass), which has been reported in the literature to be an important mechanism in As fixation [18,19], failed to improve the levels of As immobilisation and actually caused a slight enhancement in As solubility. Other results reported by the authors suggested a slight association between As and the Fe_2O_3 present in fly ash but not in externally added Fe_2O_3 [23].

3.3 Microstructure and crystalline phases in control and Cs doped AAFA.

From the XRD data shown in Figure 3, the formation of two new zeolite phases (herchelite and hydroxysodalite) is clearly evident. The crystalline phases in the original fly ash (mullite and quartz) did not react during the alkali activation process. However, important changes are noted in the broad background hump between 15 and 35 degrees 2 Theta. This area corresponds to the amorphous vitreous material present in the fly ash and significant changes in this region confirm the reaction of the glassy phase in accordance with the widely accepted theories of fly ash activation [36,37].

A probable immobilisation mechanism for Cs in the AAFA system is by incorporation into zeolite structures during paste hardening. It is likely that the substitution of Na^+ for Cs^+ would provoke some slight changes in crystal unit structures, and thus diffraction patterns, due to the considerable differences in ionic radii of the two cations.

Comparing the diffraction patterns for control AAFA and Cs-doped AAFA, the zeolite peaks are very similar in both position and intensity. The only notable changes following addition of Cs were that the Herchelite peak at 16 degrees disappeared and that the peaks at 23, 34 and 36 degrees became less intense relative to the rest of the spectra. Other authors in the literature have also reported relatively few changes in diffraction patterns of zeolites with Cs^+ substituting for Na^+ [38,39]. It must also be noted that the relatively low content of Cs (1%) may make the appearance of any new, Cs containing crystalline phases difficult to detect by the XRD technique.

From the SEM data in Figure 4, the widespread formation of zeolite crystal structures is evident. Also evident is the XRD amorphous N-A-S-H type gel (see image b), which is generally considered to be liable to crystallise into zeolitic phases over longer periods of time.

A number of microanalyses were also carried out to determine elemental composition, especially Cs content, at specific points in the paste samples. However, at no point was any site found which Cs was concentrated significantly higher than the 1% dosage by which it was added. In general, traces of Cs were found in almost all locations, implying that the Cs^+ ion is incorporated into the paste in both amorphous N-A-S-H gel and precipitated zeolite structures at low concentrations. Where ion exchange mechanisms determine the substitutions between Cs^+ and Na^+, Cs^+ will show a stronger affinity for the exchange site due to its larger ionic radius. The effects of changing the curing time and of changing the Cs salt used have been presented in another paper by the authors [40].

3.4 Elemental distribution of Hg in Hg doped AAFA matrix.

The Hg-doped AAFA pastes were the only samples to show visible evidence of a specific metal containing product. During mixing, very small yellow patches would appear in the pastes from time to time. This could be expected to be HgO, whose formation is expected in a highly alkaline environment [10]. Later, in the hardened paste, a very small number of orange precipitates could be seen by eye in paste fracture surfaces. An SEM/EDX examination of one of these precipitates is given in Figure 5.

The elemental distribution data as per the line scan in Figure 5 reveal that the orange precipitate is particularly rich in Hg and S compared to expected background levels. As no sulphur containing compound was added to the mixture, this must be present as impurities in the starting fly ash. Part b) of Figure 5 indicates that there are two distinct zones in the SEM image (separated by a dotted line). To the left of the line, where the orange precipitate exists, the spectra is dominated by S and Hg. To the right of the line, Hg and S contents decrease but Al and Si levels increase, implying the transition to an area of the paste more dominated by N-A-S-H gel than Hg.

Although the elemental spectra in part b) imply that S is the dominant element, the EDX data given in part c) show that, across the entire line, Hg and O were the dominant elements. Therefore the Hg precipitate is associated with both S and O. This gives rise to the orange precipitate being either HgS, Hg_2S (both highly insoluble), $HgSO_4$ (soluble) or a combination of HgS/Hg_2S and HgO (sparingly soluble).

Taking into consideration that >99% of Hg was immobilised according to the TCLP test, the existence of $HgSO_4$ at high levels can be excluded as it is a soluble salt. The orange colour of the precipitate matches well with HgO (which exists as yellow or red allotropes) but could also fit well with HgS (a red coloured compound). Accounting for the average Hg:S atomic ratio of 31:9 given in part c) of Figure 5, it is clear that not all Hg could exist as HgS or even Hg_2S. The most likely explanation is that a combination of HgO and HgS/Hg_2S is present.

In XRD analysis (not included) no new peaks attributable to HgO, HgS or Hg_2S were noted. However, this could be due to the semi-crystalline nature of the precipitate (see part d of Figure 5) and/or the fact that only a small percentage of Hg was present in the sample. Other published work on this subject stated that even with 5% Hg addition, no new crystalline phases were noticed except for NaCl, due to reaction of the Cl^- from the Hg salt and Na^+ from the NaOH activator [27]. In the same paper, Hg precipitates also show a poorly crystalline morphology.

3.5 Microstructure and crystalline phases in control and As-doped AAFA

The largest reductions in mechanical strengths were noted in the As-doped pastes. Therefore it was decided to analyse the control and As-doped pastes for total porosity and pore size distribution in order to determine if As addition was significantly affecting the paste microstructure. Mercury intrusion porosimetry results are given in Figure 6.

A number of points can be drawn from the data presented in Figure 6. First of all, it is clear that the addition of either Fe or As causes a slight increase in total porosity. The addition of both together increased total porosity further still, which is logical considering the dilution effect of replacing “cementing” material with “non-cementing” material.

The addition of Fe alone caused the most significant increase in large pores (100-200μm). The specific effect of adding As was to provoke an increase in larger pores (>10μm) at the expense of pores <10μm. The porosity data is consistent with the reductions in mechanical strengths observed in Figure 2 with As-doped pastes.

From Figure 7 it is evident that both zeolite type phases, as observed in Figures 3 and 4, and non-crystalline N-A-S-H type gel are formed in As-doped AAFA pastes. Due to the poor immobilisation performance of As, it is likely that a significant fraction of As remains in the pore solution and thus would not be found in freeze dried pastes.

The ca. 50% As that remained with paste solids following the TCLP test is most likely to be reversibly absorbed at cation exchange sites on the zeolite phases. Previous work by the authors has revealed that in dynamic leaching tests, virtually all As is eventually leached [40]. Such behaviour implies that no strong affinity for As is demonstrated by the zeolite phases (mainly of the herchelite and hydroxysodalite types) formed in the As-doped AAFA.

In micro-analyses (not included) no major enrichment in As content could be found at Fe_2O_3 grain surfaces. This was to be expected given the particularly poor TCLP results for the Fe + As treated AAFA paste. One possibility is that the surface chemistry of sites on Fe_2O_3 grains does not show a high affinity for As in a highly alkaline environment. Another possibility is that the Fe_2O_3 used in this study was extremely well ordered or had a relatively small surface area. Regardless, the main conclusion is that As immobilisation was unsatisfactory under the conditions studied.

4 Conclusions

This work has focussed on the immobilisation of three metals (Cs, Hg and As) which are not well immobilised in Portland cement based cements. As an alternative to Portland cement immobilisation, we have investigated the potential of a completely different cementitious matrix, based on alkali activated fly ashes. The chemistry of AAFA cements is significantly different to that of Portland cement in that a N-A-S-H type gel is formed instead of C-S-H type gel and that zeolite formation is favoured.

From the results presented, it can be concluded that AAFA cements show considerable promise in the immobilisation of Cs and Hg, but not with As. The favourable results in Cs and Hg immobilisation in AAFA cements reported here, in combination with a number of other promising results published elsewhere for other metals, mean that AAFA cements should continue to gain importance in the field of solid waste management.

In the case of Cs^+, both the N-A-S-H type gel and the zeolite phases formed in-situ can act as potential immobilisation sites by substitution of Na^+ for Cs^+.

In Hg-doped pastes, the precipitation of Hg rich compounds was clearly visible both by eye and under SEM. It is likely that a combination of HgO (sparingly soluble) and HgS/Hg_2S (highly insoluble) are formed.

Finally, with As-doped pastes, poor immobilisation performance was observed both with and without the addition of Fe_2O_3 as an immobilisation aid. The unexpectedly poor performance of the Fe_2O_3 samples is linked both to an increase in total sample porosity and perhaps also to the fact that the type of Fe_2O_3 chosen was not particularly suitable either due to its fineness or surface chemistry in high pH environments.

References

[1] Palomo A., Grutzeck M.W. and Blanco M.T. Alkali-activated fly ashes. A cement for the future. *Cement and Concrete Research*, Vol 29, 1999, pp 1323-1329.

[2] Palomo A., Alonso S. and Fernández-Jiménez A. Alkaline activation of fly ashes: NMR study of the reaction products. *Journal of the American. Ceramic Society*, Vol 87, No 6, 2004, pp 1141-1145.

[3] Bakharev, T. Geopolymeric materials prepared using class F fly ash and elevated temperature curing. *Cement and Concrete Research*, Vol 35, No6, 2005, pp 1224-1232.

[4] Rees C.A., Provis J.L., Lukey G.C. and Van Deventer J.S.J. The mechanism of geopolymer gel formation investigated through seeded nucleation. *Colloids and Surfaces A: Physicochemical and Engineering Aspects*, Vol 318, No 1-3, 2008, pp 97-105.

[5] Oh J.E., Monteiro P.J.M., Jun S.S., Choi S., and Clark S.M. The evolution of strength and crystalline phases for alkali activated ground blast furnace slag and fly ash based geopolymers. *Cement and Concrete Research*, Vol 40, No 2, 2010, pp 189-196.

[6] USEPA Test Method 1311-1–TCLP, Toxicity Characteristic Leaching Procedure—1992 revision.

[7] BS EN 12457-2, Characterisation of Waste-Leaching-Compliance Test for Leaching of Granular Waste Materials and Sludges, British Standards Institute, 2002.

[8] Bagosi S. and Csetenyi L.J. Immobilization of caesium-loaded ion exchange resins in zeolite-cement blends. *Cement and Concrete Research*, Vol. 29, 1999, pp 479-485.

[9] Garrett A. and Hirschler A.E. The solubilities of red and yellow mercuric oxides in water, in alkali, and in alkaline salt solutions. The acid and basic dissociation constants of mercuric hydroxide, *Journal of the American Chemical Society*, Vol 60, 1938, pp 299–306.

[10] McWhinney H.G., Cocke D.L., Balke K. and Dale Ortego, J. An investigation of Mercury solidification and stabilization in Portland cement using X-Ray photoelectron spectroscopy and energy dispersive spectroscopy. *Cement and Concrete Research*, Vol. 20, 1990, pp 79-91.

[11] Hamilton W.P. and Bowers A.R. Determination of acute Hg emissions from solidified/ stabilized cement waste forms, *Waste Management,* Vol 17, 1997, pp 25–32.

[12] Poon C.S., Peters C.J. and Perry R. Mechanisms of metal stabilization by cement based fixation processes. *The Science of the Total Environment*, Vol. 41, 1985, pp 55-71.

[13] Shively W., Bishop P., Gress, D. and Brown T., Leaching Test of Heavy Metals Stabilized with Portland Cement, *Journal of the Water Pollution Control Federation*, Vol. 58, No 3, 1986, pp 234-241.

[14] Kyle J.H. and Lunt D. An Investigation of Disposal Options for As_2O_3 Produced from Roasting Operations, *Proceedings of the 5th Extractive Metallurgy Conference*, Perth, Australia, 1991, pp. 347–353.

[15] Dutré V. and Vandecasteele C. An evaluation of the solidification/stabilisation of industrial arsenic containing waste using extraction and semi-dynamic leach tests. *Waste Management*, Vol 16, 1996, pp 625-631.

[16] Mambote R.C.M., Reuter M.A., Van Sandwijk A. and Krijgsman P. Immobilization of Arsenic in Crystalline Form from Aqueous Solution by Hydrothermal Processing above 483.15K, *Minerals Engineering*, Vol 14, No 4, 2001, pp 391–403.

[17] [Singh T.S. and Pant K.K. Solidification/stabilization of arsenic containing solid wastes using Portland cement, fly ash and polymeric materials. *Journal of Hazardous Materials*, Vol 131, 2006, pp 29-36.

[18] Seidel H., Gorsch K., Amstatter K. and Mattusch J. Immobilization of arsenic in a tailings material by ferrous iron treatment. *Water Research*, Vol 39, 2005, pp 4073-4082.

[19] Li Y., Wang J., Peng X., Ni F. and Luan, Z.. Evaluation of arsenic immobilization in red mud by CO_2 or waste acid acidification combined ferrous (Fe^{2+}) treatment. *Journal of Hazardous Materials*, Vol 199-200, 2012, pp 43-50.

[20] Van Jaarseveld J.G.S., Van Deventer J.S.J. and Schwartzman A. The potential use of geopolymeric materials to immobilise toxic metals: Part II. Material and leaching characteristics, *Minerals Engineering*, Vol 12, 1999, pp 75–91.

[21] Palomo A. and López de la Fuente J.I. Alkali-activated cementitious materials: alternative matrices for the immobilisation of hazardous wastes: Part I. Stabilisation of boron, *Cement and Concrete Research*. Vol 33, 2003, pp 281–288.

[22] Palomo A. and Palacios M. Alkali-activated cementitious materials: alternative matrices for the immobilisation of hazardous wastes: Part II. Stabilisation of chromium and lead, *Cement and Concrete Research*, Vol 33, 2003, pp 289–295.

[23] Fernández-Jiménez A., Lachowski E.E., Palomo A. and Macphee D.E. Microstructural characterisation of alkali-activated PFA matrices for waste immobilisation. *Cement and Concrete Composites*, Vol 26, 2004, pp 1001-1006.

[24] Fernández-Jiménez A., Macphee D.E., Lachowski E.E. and Palomo, A. Immobilization of cesium in alkaline activated fly ash matrix. *Journal of Nuclear Materials*, Vol 346, 2005, pp 185-193.

[25] Xu J.Z., Zhou Y.L., Chang Q. and Qu, H.Q. Study on the factors affecting the immobilization of heavy metals in fly ash-based geopolymers, *Materials. Letters*. Vol 60, 2006, pp 820–822.

[26] Shi C. and Fernández-Jiménez A. Stabilization/solidification of hazardous and radioactive wastes with alkali-activated cements, *Journal of Hazardous Materials*, Vol B137, 2006, pp 1656–1663.

[27] Donatello S., Fernández-Jiménez, A. and Palomo, A. An assessment of Mercury immobilisation in alkali activated fly ash (AAFA) cements. Journal of Hazardous Materials, Vol 213-214, 2012, pp 207-215.

[28] Querol X., Moreno N., Umaña J.C., Alastuey A., Hernández E., López-Soler A. and Plana F. Synthesis of zeolites from coal fly ash: an overview. *International Journal of Coal Geology*, Vol 50, No 1-4, 2002, pp 413-423.

[29] Sinha, P.K., Panicker P.K., Amalraj R.V. and Krishnasamy V. Treatment of radioactive liquid waste containing caesium by indigenously available synthetic zeolites: A comparative study. *Waste Management,* Vol 15, 1995, pp 149-157.

[30] Xu Y., Nakajima T. and Ohki A. Adsorption and removal of arsenic (V) from drinking water by aluminium-loaded Shirasu-zeolite. *Journal of Hazardous Materials*, Vol 92, 2002, pp 275-287.
[31] Dyer A., Chimedtsogzol A., Campbell L. and Williams C. Uptake of caesium and strontium radioisotopes by natural zeolites from Mongolia. *Microporous and Mesoporous Materials*, Vol 95, 2006, pp 172-175.
[32] Somerset V., Petrik, L. and Iwuoha, E. Alkaline hydrothermal conversion of fly ash precipitates into zeolites 3: The removal of mercury and lead ions from wastewater. *Journal of Environmental Management*, Vol 87, No 1, 2008, pp 125-131.
[33] Chutia P., Kato S., Kojima T. and Satokawa S. Arsenic adsorption from aqueous solution on synthetic zeolites. *Journal of Hazardous Materials*, Vol 162, 2009, pp 440-447.
[34] Zhang X.Y. Wang Q.C., Zhang, S.Q., Sun X.J. and Zhang Z.S. Stabilization/solidification (S/S) of mercury-contaminated hazardous wastes using thiol-functionalized zeolite and Portland cement. Journal of Hazardous Materials, Vol 168, No 2-3, pp 1575-1580.
[35] Camacho L.M., Parra R.R. and Deng S. Arsenic removal from groundwater by MnO_2-modified natural clinoptilolite zeolite: Effects of pH and initial feed concentration. *Journal of Hazardous Materials*, Vol 189, 2011, pp 286-293.
[36] Davidovits J, Geopolymers. Inorganic polymeric new materials. *Journal of Thermal Analysis*, Vol 37, 1991, pp 1633-1656.
[37] Provis J.L. Geopolymers: structure, processing, properties and industrial applications.2009, CRC Press, Oxford.
[38] Hoyle S.L. and Grutzeck M.W. Incorporation of cesium by hydrating calcium aluminosilicates, *Journal of the American Ceramic Society*, Vol 72, No 10, 1989, pp 1938-1947.
[39] Lambregts M.J. and Frank S.M. Characterization of cesium containing glass-bonded ceramic waste forms. *Microporous, & Mesoporous Materials*, Vol 64, No 1-3, 2003, pp 1-9.
[40] Fernández-Jiménez A., Palomo A., MacPhee D.E. and Lachowski E.E. Fixing arsenic in alkali-activated cementitious matrices, *Journal of the American Ceramic Society*, Vol 88, 2005, pp 1122–1126.

Table 1. Test mixture compositions.

Sample ID	**FA**	**$CsOH.H_2O$**	**$HgCl_2$**	**$NaAsO_2$**	**Fe_2O_3**	**Curing temp.**	**Curing time**
Control-1	100%					85°C	7d
Control-2	100%					85°C	20h
Control-Fe	95%				5%	85°C	20h
Cs	98.74%	1.26%				85°C	7d
Hg	99.32%		0.68%			85°C	20h
As	98.25%			1.75%		85°C	20h
As-Fe	93.25%			1.75%	5%	85°C	20h

*Cs, Hg and As salt additions are equivalent to 10000, 5000 and 10000ppm respectively

Table 2. TCLP immobilisation efficiencies.

	Cs	**Hg**	**As**	**As-Fe**
Immobilisation efficiency (%)	99.7%	99.3%	50.8%	44.9%

Fig. 1 Illustration of the alkali activation process.

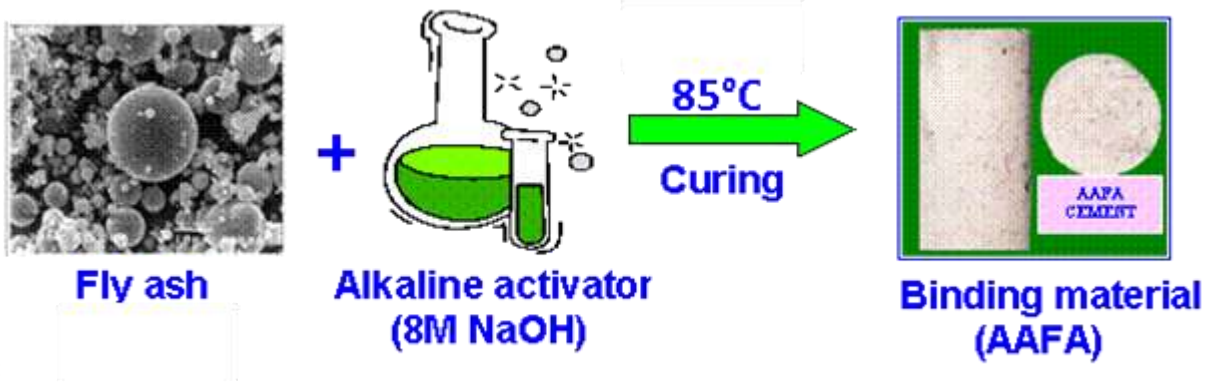

Fig. 2 Effect of metal addition on flexural and compressive strengths relative to control cement strengths.

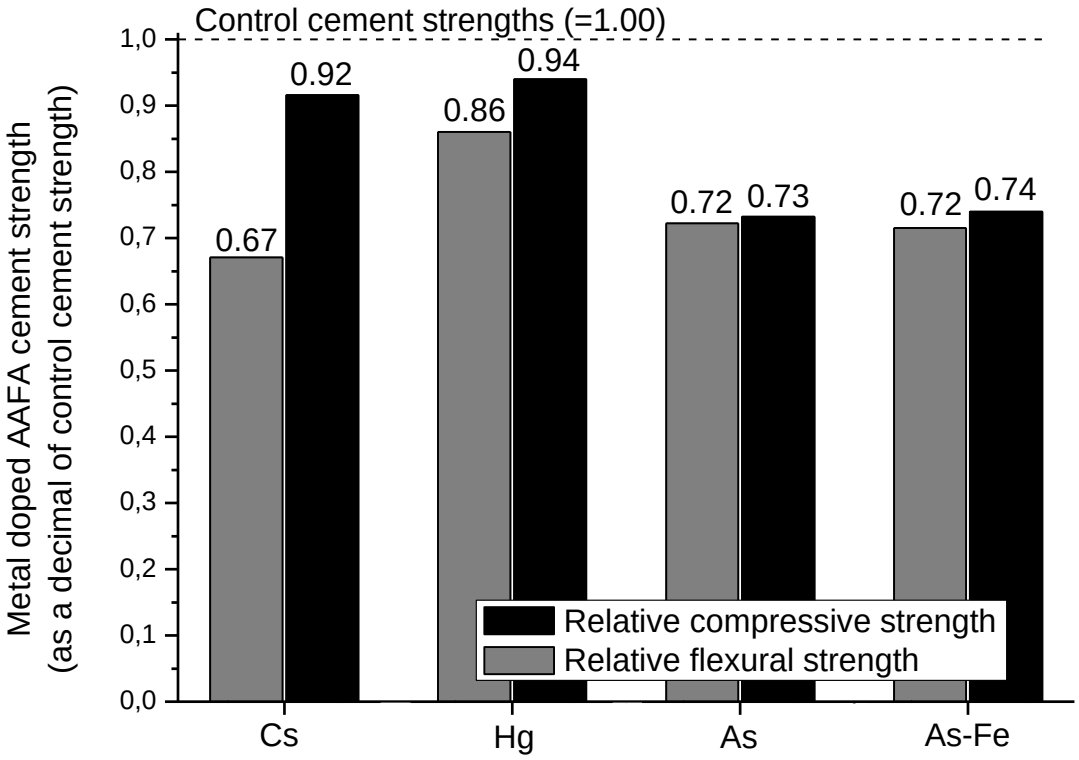

Fig. 3. XRD data for fly ash (bottom), control AAFA cement (middle) and Cs-doped AAFA cement (top).

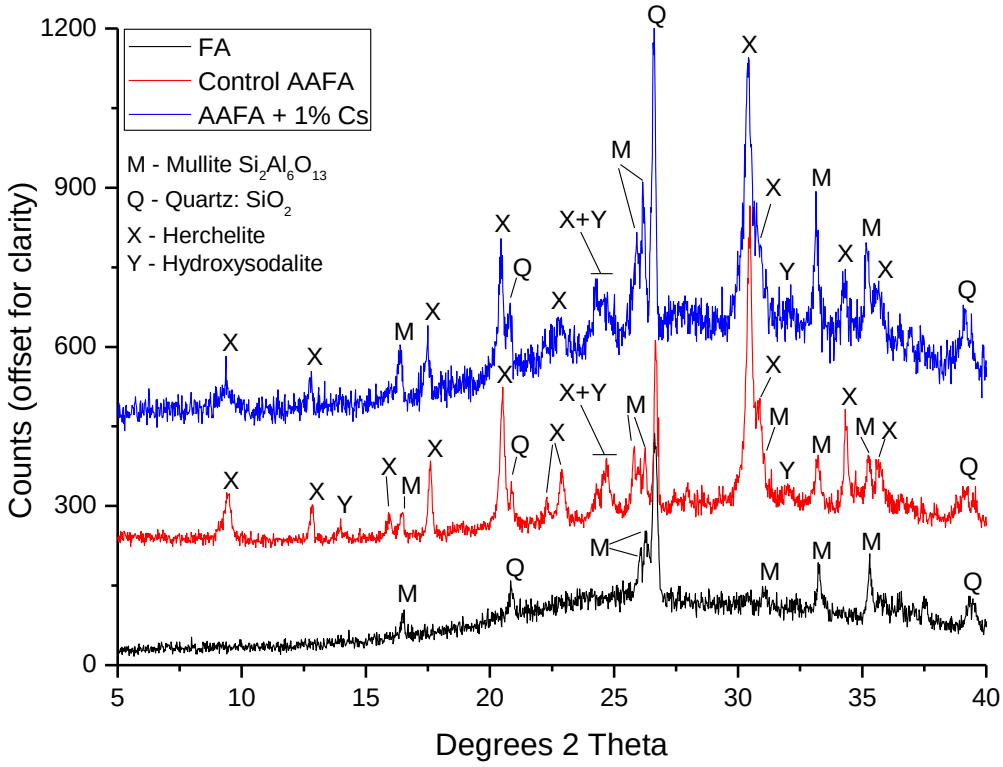

Fig. 4 SEM analysis of Cs-doped AAFA microstructure: a) general overview, b) amorphous gel and c) zeolite crystals precipitated in a pore cavity.

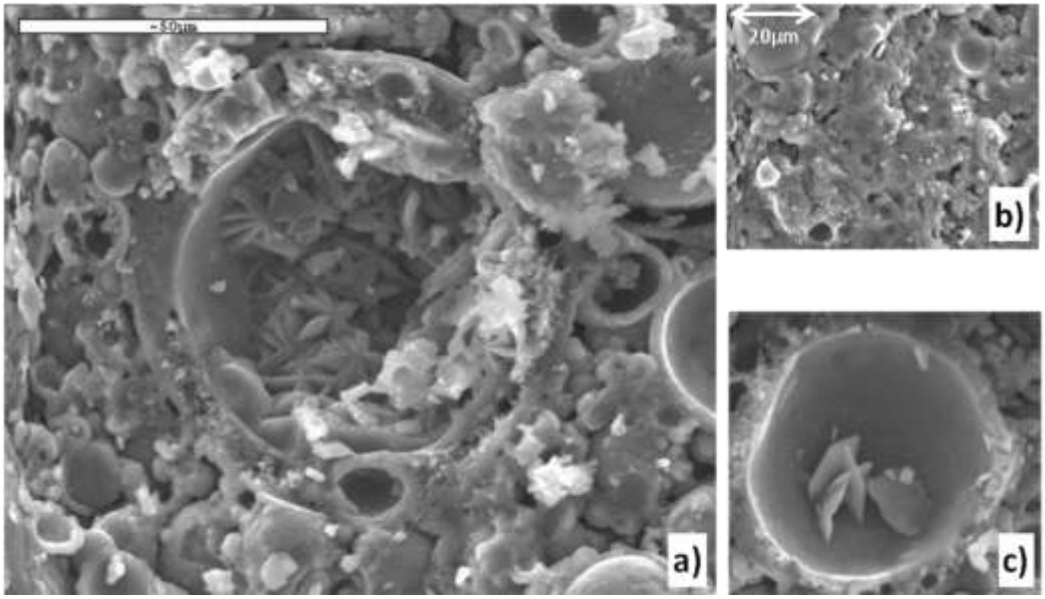

Fig. 5 a) SEM image of a zone containing an orange precipitate originally thought to be HgO, b) elemental distribution of a line scan drawn across the precipitate region, c) Average EDX spectra and atomic % data for all points on the line scan and d) a closer look at Hg precipitate morphology.

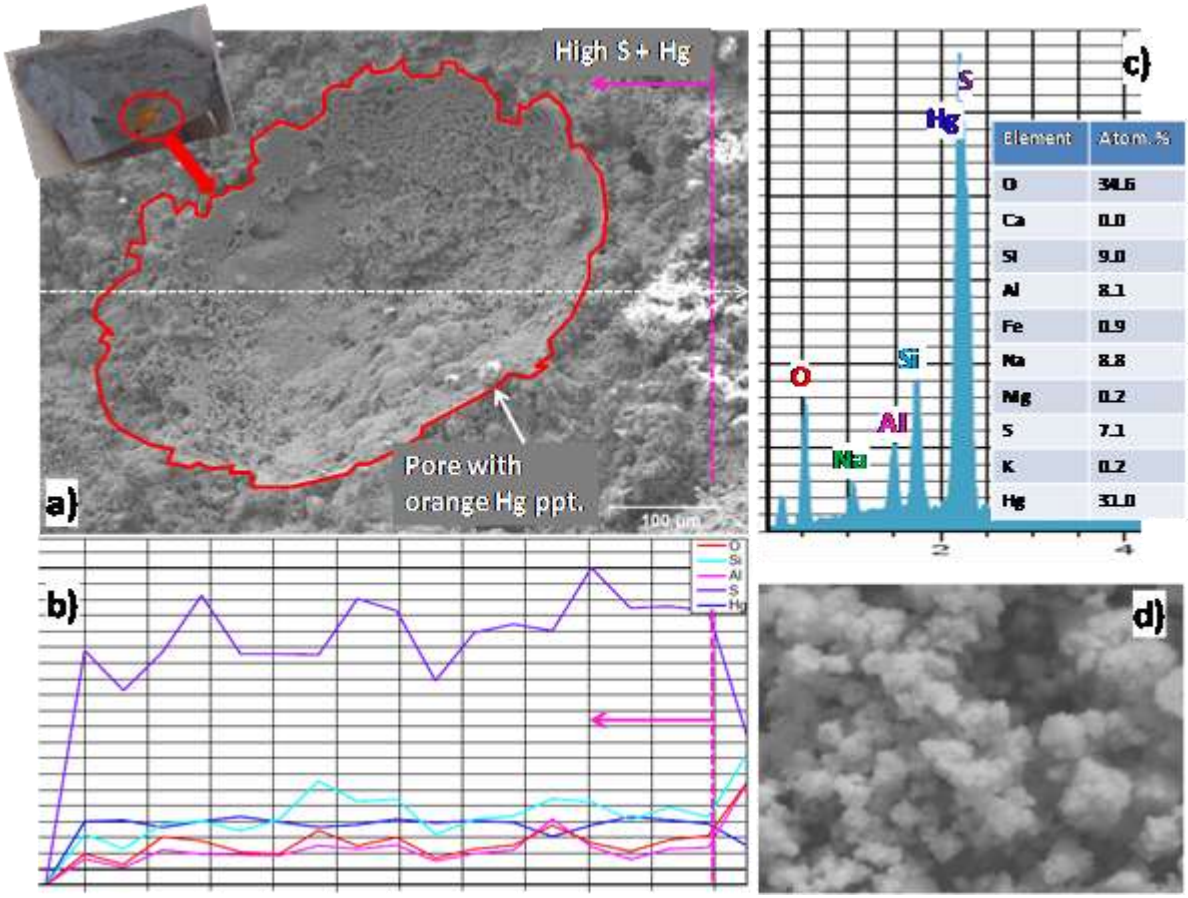

Fig. 6 Effect of Fe and As addition on total porosity and pore size distributions of AAFA pastes.

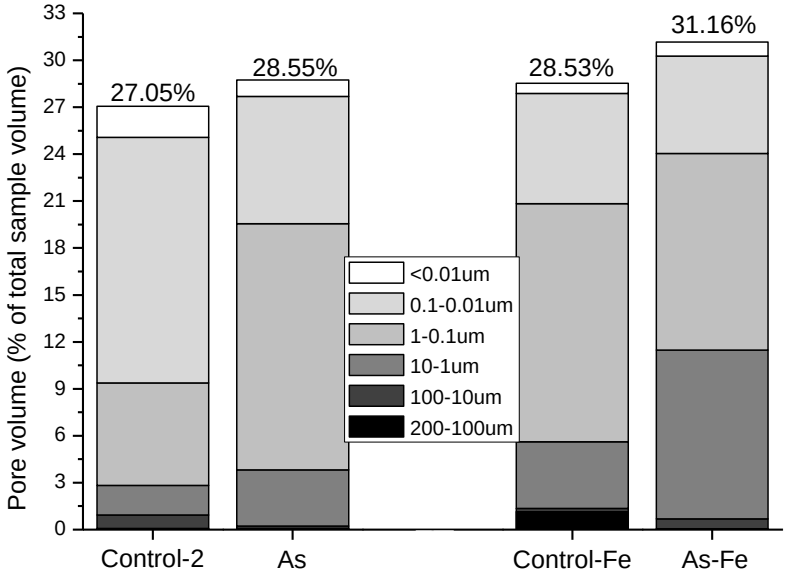

Fig. 7. SEM image of As-doped AAFA cement.

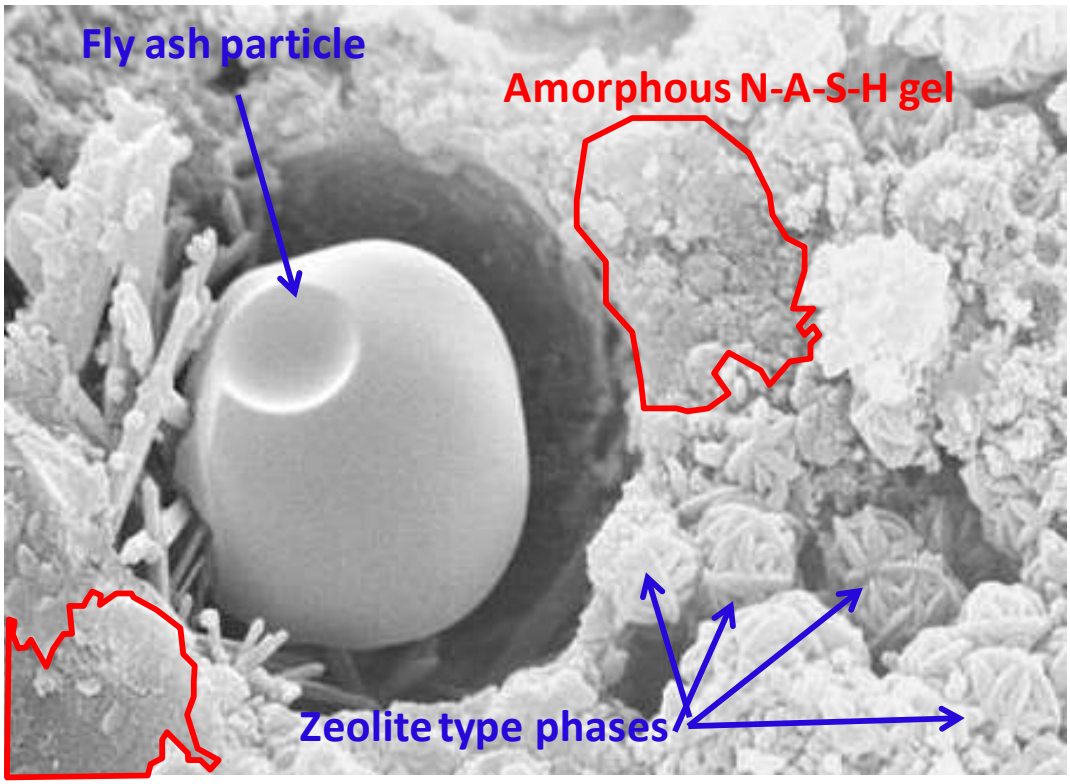

Contact address:

Dra. Ana Fernández
Instituto de Ciencias de la Construcción Eduardo Torroja (CSIC)
Dpto. Cementos y Reciclado de Materiales
Tfno.: +34 91 3020440 (ext 217)
Fax.: +34 91 3026047
e-mail.: anafj@ietcc.csic.es